Published in final edited form as:
Dev Dyn. 2014 March ; 243(3): 440–450. doi:10.1002/dvdy.24090.

Conditional ablation of *Tbr2* results in abnormal development of the olfactory bulbs and subventricular zone-rostral migratory stream

Robert J. Kahoud[1,2,#], **Gina E. Elsen**[2,^], **Robert F. Hevner**[2,3,*], and **Rebecca D. Hodge**[2,3,*]

[1]Division of Pediatric Critical Care Medicine, University of Washington and Seattle Children's Hospital, M/S W-8866, 4800 Sand Point Way NE, Seattle, WA, 98105, USA

[2]Center for Integrative Brain Research, Seattle Children's Research Institute, M/S C9S-10, 1900 Ninth Avenue, Seattle, WA, 98101, USA

[3]Department of Neurological Surgery, University of Washington, Seattle, WA, 98195, USA

Abstract

Background—Development of the olfactory bulb (OB) is a complex process that requires contributions from several progenitor cell niches to generate neuronal diversity. Previous studies showed that *Tbr2* is expressed during the generation of glutamatergic OB neurons in rodents. However, relatively little is known about the role of *Tbr2* in the developing OB or in the subventricular zone-rostral migratory stream (SVZ-RMS) germinal niche that gives rise to many OB neurons.

Results—Here, we use conditional gene ablation strategies to knockout *Tbr2* during embryonic mouse olfactory bulb morphogenesis, as well as during perinatal and adult neurogenesis from the SVZ-RMS niche, and describe the resulting phenotypes. We find that *Tbr2* is important for the generation of mitral cells in the OB, and that the olfactory bulbs themselves are hypoplastic and disorganized in *Tbr2* mutant mice. Furthermore, we show that the SVZ-RMS niche is expanded and disordered following loss of *Tbr2*, which leads to ectopic accumulation of neuroblasts in the RMS. Lastly, we show that adult glutamatergic neurogenesis from the SVZ is impaired by loss of *Tbr2*.

Conclusions—*Tbr2* is essential for proper morphogenesis of the OB and SVZ-RMS, and is important for the generation of multiple lineages of glutamatergic olfactory bulb neurons.

Keywords

Olfactory bulbs; *Tbr2*; Subventricular Zone; Rostral Migratory Stream; Neural Development

[*]**Corresponding authors:** Rebecca D. Hodge, Center for Integrative Brain Research, Seattle Children's Research Institute, M/S C9S-10, 1900 Ninth Avenue, Seattle, WA 98101. rdhodge@uw.edu. Robert F. Hevner, Center for Integrative Brain Research, Seattle Children's Research Institute, M/S C9S-10, 1900 Ninth Avenue, Seattle, WA 98101. rhevner@uw.edu.
[#]Present address: Division of Pediatric Critical Care Medicine, Mayo Clinic, Rochester, MN, 55905, USA
[^]Present address: Department of Neurology and Epileptology, Hertie Institute for Clinical Brain Research, University of T&#65533;bingen, Tübingen, D72076, Germany

Introduction

The rodent olfactory bulb (OB) contains a large diversity of neurons. Accordingly, the developmental plan of this structure is complex, and OB neurogenesis requires contributions from several different progenitor cell niches. During early embryonic development, local progenitors in the OB ventricular zone produce projection neurons for the mitral/tufted cell layer (MCL) (Blanchart et al. 2006). Interneurons that populate the granule cell and glomerular layers are produced during later embryonic and perinatal development from progenitor cells located outside of the OB in the subventricular zone (SVZ) neurogenic niche (Allen et al. 2007; De Marchis et al. 2007; Lledo & Saghatelyan 2005; Lledo et al. 2008; Winpenny et al. 2011).

The SVZ is the largest germinal niche in the postnatal brain, and SVZ progenitors continue to generate new OB neurons throughout life (Lledo & Saghatelyan 2005; Lledo et al. 2008; Whitman & Greer 2009). Within the SVZ, neural stem cells (NSC) proliferate to generate a pool of rapidly dividing intermediate neuronal progenitors (INPs) that produce multiple types of neurons, which migrate through the rostral migratory stream (RMS) to the OB. Development of the SVZ-RMS structure is itself a complex process that requires correct early morphogenesis of the OB and maturation of tangential migratory pathways in the RMS (Pencea & Luskin 2003; Peretto et al. 2005; Merkle et al. 2007). Ultimately, progenitors that remain in the adult SVZ are diverse, but somewhat lineage restricted, as different subtypes of OB interneurons are produced from distinct regions of the SVZ (Merkle et al. 2007). The cell intrinsic programs that specify fate within each lineage and their interplay with extrinsic factors that govern correct migration and positioning in the RMS and OB are not completely understood (Hodge et al. 2012a; Hsieh 2012).

The T-box transcription factor (TF) *Tbr2* regulates glutamatergic neurogenesis in multiple regions of the brain including the embryonic neocortex (Arnold et al. 2008; Sessa et al. 2008, 2010) and the developing and adult hippocampus (Hodge et al. 2012b, 2013). The transcriptional program that controls progression from NSC to INP to neuroblast in these contexts involves sequential expression of *Pax6→Neurog2→Tbr2→Tbr1* (Englund et al. 2005; Hodge et al. 2008; Roybon et al. 2009). While expression of *Tbr2* in INPs that produce mitral cells during OB development was demonstrated some time ago (Bulfone et al. 1999), only recently have *Tbr2*-expressing INPs in the dorsal SVZ been shown to produce glutamatergic OB interneurons at embryonic, perinatal (Winpenny et al. 2011), and adult stages (Brill et al. 2009; Roybon et al. 2009). However, relatively little is known about the role of *Tbr2* in regulating SVZ-RMS-OB development and ongoing glutamatergic neurogenesis from the adult SVZ. Therefore, we determined the phenotypes that result from conditional ablation of *Tbr2* in the developing and adult SVZ-RMS-OB. Our results indicate that knockout of *Tbr2* results in significant abnormalities in OB development, including near complete loss of mitral cells. Additionally, we describe a novel SVZ-RMS phenotype in *Tbr2* conditional mutants that includes expansion of the SVZ-RMS and ectopic accumulation of diverse cell types in this zone. Furthermore, we demonstrate that conditional ablation of *Tbr2* in adult mice impairs glutamatergic neurogenesis from the adult SVZ.

Results and Discussion

Tbr2 ablation results in defects in OB morphogenesis and the generation mitral cells

To determine the role of *Tbr2* in OB development, we used *Nestin*-Cre to conditionally knockout *Tbr2* in the CNS starting at embryonic day (E) 11.5 (Hodge et al. 2012b, 2013). We noted abnormalities in OB development as early as E14.5 (Fig. 1A, B). For example, in E14.5 control mice (Fig. 1A) the developing OB was readily identifiable and was undergoing significant neurogenesis as evidenced by robust expression of Doublecortin (DCX), a marker of newborn neurons (Seri et al. 2004; Couillard-Despres et al. 2005; Walker et al. 2007). Conversely, OB size was already decreased in E14.5 conditional *Tbr2* knockouts (Fig. 1B), and though DCX was present in the mutant OB, it appeared to be slightly reduced. Gross examination of the postnatal *Nestin*-Cre;*Tbr2*$^{Flox/Flox}$ brain confirmed significant OB hypoplasia in mutants in comparison to controls (Fig.1C, D, arrow). Nuclear staining with DAPI revealed general disorganization of the OB, including ill-defined plexiform layers, and, most prominently, absence of the MCL (Fig. 1E–H; note the arrow illustrating the control MCL in G and the corresponding lack of this layer in the *Tbr2* mutant in H). However, glomerular structure appeared to be somewhat preserved in the mutant OB (Fig. 1G–H, S–T).

As *Tbr2* had been previously implicated in the regulation of mitral cell development (Arnold et al. 2008; Mizuguchi et al. 2012), we examined this cell population in *Nestin*-Cre;*Tbr2*$^{Flox/Flox}$ mice. First, we assessed expression of Tbr2 protein, and found that ablation of *Tbr2* resulted in a near complete loss of protein in the OB in general (Fig. 1I, J), including in mitral cells which normally constitutively express this gene/protein. *Tbx21*, a transcription factor of the *Tbr1* subfamily, is also expressed in mitral cells during their development (Faedo et al. 2002). Accordingly, in P21 control mice, Tbx21 protein was limited to the MCL in the OB (Fig. 1K, arrow). However, in *Nestin*-Cre;*Tbr2*$^{Flox/Flox}$ animals, Tbx21 was virtually eliminated from the OB, suggesting near complete loss of mitral cells in mutant mice (Fig. 1L, arrowhead), consistent with previous reports (Arnold et al. 2008).

Previous work has shown that mitral cells express Reelin, a molecule important for directing neuronal migration in the OB (Hack et al. 2002; Hellwig et al. 2012). We examined Reelin expression in the developing and postnatal OB of *Tbr2* mutant mice and controls to further characterize how loss of *Tbr2* impacts mitral cell development. Consistent with early defects in OB morphogenesis (Fig. 1A, B), we found that Reelin expression was decreased in the mutant OB by E14.5, shortly after the peak period of mitral cell genesis (E10-E11) (Blanchart et al. 2006; Imamura et al. 2011) (Fig. 1M, N). This defect in Reelin expression in *Tbr2* mutant mice persisted to postnatal development and was specific to the OB, as Reelin expression appeared to be largely normal throughout the rest of the brain (Fig. 1O, P, dashed box). Furthermore, by postnatal day (P) 3, only a few scattered Reelin-expressing cells were present in the OB of *Tbr2* conditional knockouts (Fig. 1R), compared to robust Reelin expression in the MCL of age-matched controls (Fig. 1Q, arrow). Thus, these results confirm a major defect in mitral cell genesis following ablation of *Tbr2* expression during embryonic development. These findings are in accordance with previous studies showing a

role for *Tbr2* in directing mitral cell development (Arnold et al. 2008; Mizuguchi et al. 2012).

We also examined several markers of other OB neurons in P21 *Tbr2* conditional mutants and controls to determine if loss of *Tbr2* impacted their development (Fig. 1S–Z). Consistent with the partial preservation of the glomerular layer structure (Fig. 1S–T), we found that markers of periglomerular neurons including calretinin+, tyrosine hydroxylase (TH)+, and Pax6+ cells were all present within the OB of *Nestin*-Cre;*Tbr2*$^{Flox/Flox}$ animals and did not appear to be grossly different in number/density in comparison to age-matched controls. These results suggest that *Tbr2* specifically impacts mitral cell development, and does not directly affect the development of non-glutamatergic OB neurons, consistent with lack of expression of *Tbr2* in these lineages (Brill et al. 2009; Winpenny et al. 2011).

Ablation of *Tbr2* results in aberrant expansion of the SVZ-RMS during embryonic development

During OB development, migratory interneurons born in the SVZ travel to the OB through the RMS (Kohwi et al. 2007; Batista-Brito et al. 2008). Given the magnitude of OB hypoplasia noted in *Nestin*-Cre;*Tbr2*$^{Flox/Flox}$ mice, we hypothesized that, in addition to loss of mitral cells, there might also be a defect in morphogenesis of the SVZ-RMS in *Tbr2* mutants. Clear migration of neuroblasts from the SVZ through the RMS has been reported at E16.5 (Pencea & Luskin 2003). Thus, we began our examination of the developing SVZ-RMS at this age. At E16.5, we noted that the SVZ-RMS appeared to be expanded in *Tbr2* mutant mice and cell density in this region also appeared to be increased in comparison to age-matched controls (Fig. 2A, B). By P4 this defect in SVZ-RMS development was readily apparent in *Nestin*-Cre;*Tbr2*$^{Flox/Flox}$ mice (Fig. 2C, D, arrowhead). As illustrated by DAPI stained sagittal and coronal sections through the SVZ-RMS, the SVZ appeared enlarged and cell dense in P4 *Nestin*-Cre;*Tbr2*$^{Flox/Flox}$ mice, and the RMS appeared to be expanded (Fig. 1, compare G to H and I to J), similar to what was noted during earlier development of this structure. Therefore, these results suggest a persistent defect in SVZ-RMS morphogenesis in mice lacking *Tbr2* expression.

To further characterize the types of cells that constitute the expanded SVZ-RMS region in *Nestin*-Cre;*Tbr2*$^{Flox/Flox}$ mice, we assayed for a number of markers, both general and cell type specific. First, we examined expression of DCX, a general marker of newborn neurons, and found that the mutant SVZ-RMS contained an increased number of these cells in comparison to controls (P0.5; Fig. 3A, B compared to Fig. 3C, D). These findings suggest that neuroblasts accumulated ectopically within the expanded proximal RMS of *Tbr2* mutants. Ectopic accumulation of neuroblasts persisted in *Nestin*-Cre;*Tbr2*$^{Flox/Flox}$ mice, as evidenced by continued amassing of DCX+ cells in the P21 mutant SVZ-RMS (Fig. 3E, F, H, I). We also noted an apparent increase in GFAP staining (i.e. astrocytes and/or stem/progenitor cells) in the expanded RMS of *Nestin*-Cre;*Tbr2*$^{Flox/Flox}$ mice, indicating that heterogeneous cell populations were contained within the abnormal RMS of mutant mice (Fig. 3E, G, H, J).

To determine if specific types of migrating interneurons were accumulating and contributing to cellular heterogeneity within the *Tbr2* mutant SVZ-RMS we first examined a *Tbr2*^{LacZ}

knock-in mouse in which cells derived from *Tbr2*+ progenitors transiently express β-galactosidase (β-gal), thereby allowing for short-term lineage tracing of these cells (Fig. 3K, L). In control animals (P0.5), β-gal+ cells lined the dorsal compartment of the SVZ and extended along the dorsal aspect of the RMS to the core of the OB (Fig. 3K, black arrows). The MCL of control animals also contained β-gal+ cells, which were likely early born neurons that constitutively express *Tbr2* (Fig. 3L, black arrowheads) [5]. In age-matched *Nestin*-Cre;*Tbr2*$^{Flox/LacZ}$ animals, β-gal+ cells were displaced to the interior of the RMS and formed abnormal bands and clusters (Fig. 3L, arrows). Although there were some β-gal+ cells present in the mutant OB at P0.5, they were centrally located, scattered, and disorganized (Fig. 3L, arrowheads).

Next, we examined calretinin expression in *Nestin*-Cre;*Tbr2*$^{Flox/Flox}$ animals and controls to determine if *Tbr2* ablation resulted in accumulation of inhibitory interneurons in the SVZ-RMS (Fig. 3M–T). Peak inhibitory interneuron production from the SVZ occurs during the first postnatal week (Batista-Brito et al. 2008); therefore, we examined calretinin staining in control and mutant animals at P3. Control animals had numerous tangentially oriented calretinin+ cells in the RMS (Fig. 3M–O), and in the OB, calretinin+ cells were radially oriented in the granule cell layer and dispersed through the glomerular layer (Fig. 3M, P). In P3 *Nestin*-Cre;*Tbr2*$^{Flox/Flox}$ mice, increased calretinin+ cells were noted in the RMS (Fig. 3Q–S). These calretinin+ cells appeared disorganized in the proximal RMS, and were increased in number in comparison to control mice (Fig. 3R). In the distal RMS of *Nestin*-Cre;*Tbr2*$^{Flox/Flox}$ mice, calretinin+ neuroblasts were present in large clusters, a phenomenon that was not observed in control animals (Fig. 3S, arrows). Although some calretinin+ cells were found in the OB of mutant mice, they were disorganized, as evidenced by their lack the clear radial orientation in the granule cell layer, a feature that was observed in control mice (Fig. 3S, T).

Considering that the large accumulation of cells in the aberrant SVZ-RMS of *Tbr2* mutants may prevent these cells from migrating to and integrating into the OB, we hypothesized that increased cell death may be expected to occur. Thus, we examined *Nestin*-Cre;*Tbr2*$^{Flox/Flox}$ mice and controls for indications of apoptosis by immunostaining for activated Caspase-3 (Fig. 4). Increased cell death was noted in the OB of *Nestin*-Cre;*Tbr2*$^{Flox/Flox}$ mice at P3, as well as throughout the expanded SVZ-RMS (Fig. 4A–B1, C–D1). These results suggest that aberrant SVZ-RMS-OB morphogenesis following ablation of *Tbr2* results in increased apoptosis in mutant mice. Consistent with this notion, we found that the size of the SVZ-RMS decreased over time in *Tbr2* knockout mice. For example, the SVZ-RMS was still expanded in mutant mice compared to controls at P21 (Fig. 3E, H), but to a lesser degree than what was observed at P0.5 and P3 (Fig. 3, Fig. 5). Accordingly, we found that the expansion of the SVZ-RMS was notably reduced by P60 in *Tbr2* knockout mice (Fig. 4E, F). In fact, when we examined 4 month old (P120) *Nestin*-Cre;*Tbr2*$^{Flox/Flox}$ mice and age-matched controls, we found that expansion of the SVZ-RMS in mutants was largely resolved, as by this age the RMS appeared only slightly wider than normal (Fig. 4I, J). However, while the size of the SVZ-RMS decreases over time in *Tbr2* knockout mice, the structure of the SVZ-RMS remains abnormal as evidenced by the fact that the RMS does not appear to connect to the OB in these older mutants (Fig. 4E, F, I, J). Importantly, OB

hypoplasia continued to be apparent in 4 month old *Nestin*-Cre;*Tbr2*$^{Flox/Flox}$ animals, indicating that the decreased expansion of the SVZ-RMS in older *Tbr2* mutant mice likely did not result from increased migration of cells to the OB (Fig. 4G, H).

These results imply that most of the ectopic cells in the SVZ-RMS of younger mice do not survive through the development and maturation period of this structure. Interestingly, in a previous study of conditional *Tbr2* knockout mice, development of the SVZ-RMS was reported to be unaffected by loss of *Tbr2* (Arnold et al. 2008). However, this previous study made use of *Sox1*-Cre to ablate *Tbr2*, which has a different expression pattern than the *Nestin*-Cre that we have used in the present report (Takashima et al. 2007; Tronche et al. 1999). Furthermore, in the previous study by Arnold et al. (2008) the SVZ-RMS was only examined at P60, at which time it reportedly appeared normal in mutant mice. As we show that defects in the SVZ-RMS are somewhat resolved in our older mice (P60-P120), it is possible that by P60 a defect in the SVZ-RMS might not have been obvious in *Sox1*-Cre;*Tbr2*$^{Flox/Flox}$ mutants, which may explain the apparent discrepancy between the SVZ-RMS phenotypes described in these studies. While our results indicate that disrupted migration of neuroblasts through the SVZ-RMS to the OB, and subsequent death of these ectopic cells, likely contributes to the decreased OB size that we observed in *Tbr2* knockout mice, it is also possible that defects in OB innervation may contribute to the mutant OB phenotype. Several studies have shown that axons extending from olfactory sensory neurons in the olfactory epithelium that innervate the OB early in development regulate the proliferation of progenitor cells in the OB and influence OB morphogenesis (Gong et al., 1995; Shaker et al., 2012). As we have not directly examined innervation of the OB in *Tbr2* knockout mice, we cannot determine with the present study whether defects in this process contribute to the OB phenotype in mutants, but such experiments would be possible in future studies.

Differential requirement for *Tbr2* during embryonic/perinatal and adult neurogenesis from the SVZ-RMS

Tbr2 expression during glutamatergic neurogenesis has been described in several regions of the CNS, where *Tbr2* has largely been implicated in regulating neuronal fate commitment and glutamatergic differentiation (Arnold et al. 2008; Sessa et al. 2008, 2010; Hodge and Hevner 2011; Hodge et al. 2012b, 2013; Elsen et al. 2013) . For example, *Tbr2* was previously shown to be necessary for glutamatergic neurogenesis in the developing and adult Dentate Gyrus (Hodge et al. 2012b, 2013). Hence, we investigated the requirement for *Tbr2* during glutamatergic neurogenesis from the embryonic/perinatal and adult SVZ (i.e. during the generation of external tufted and short-axon cells, respectively). Tbr1 was used as a general marker of glutamatergic neuroblasts in the RMS (Brill et al. 2009; Winpenny et al. 2011). To examine the requirement for *Tbr2* during embryonic and perinatal glutamatergic neurogenesis, Tbr1 expression was assayed in *Nestin*-Cre;*Tbr2*$^{Flox/Flox}$ animals and age-matched controls from E16.5 to P21 (Fig. 5). Tbr1+ cells were present in the developing RMS of control animals as early as E16.5 (Fig. 5A, arrows), and their smaller, elongated nuclei and frequent coexpression of the neuroblast marker DCX distinguished these migratory cells from the Tbr1+ nuclei of mature neurons in the nearby cerebral cortex and anterior olfactory nuclei (Fig. 5E, G). In control mice, Tbr1+ cells were localized along the

dorsal axis of the SVZ through the RMS and into the OB at all ages examined (Fig. 5A, C, E, G, I, K). In *Nestin*-Cre;*Tbr2*$^{Flox/Flox}$ animals, Tbr1+ neuroblasts were present in the RMS at E16.5; however, they were ectopically localized to the interior of the RMS (Fig. 5B, arrows). By P0.5, Tbr1+ cells had accumulated in the RMS of mutant mice, consistent with expansion of this region as described previously (Fig. 5D, F, H), and many of these Tbr1+ cells coexpressed the neuroblast marker DCX suggesting that they were migratory neuroblasts (Fig. 5H). Tbr1+ cells continued to accumulate in the expanded RMS of *Nestin*-Cre;*Tbr2*$^{Flox/Flox}$ mice at P3 (Fig. 5J). These data suggest that *Tbr2* is not required for the generation of glutamatergic neuroblasts from the SVZ during embryonic and perinatal development, as Tbr1+ neuroblasts were present in the RMS during this time. However, by P21 (Fig. 5L) very few Tbr1+ neuroblasts remained in the RMS of *Tbr2* mutant mice, indicating that as the SVZ-RMS matures and different subtypes of glutamatergic neurons are produced, the requirement for *Tbr2* may change.

Accordingly, we next examined the requirement for *Tbr2* in the generation of glutamatergic (Tbr1+) neuroblasts from the adult SVZ-RMS. To specifically ablate *Tbr2* in the adult brain we used the tamoxifen-inducible Cre-driver *Nestin*-CreER^{T2} in combination with our *Tbr2*^{Flox} allele (i.e. *Nestin*-CreER^{T2};*Tbr2*$^{Flox/Flox}$; Fig. 5M). Adult animals were 8-weeks-old at the onset of tamoxifen treatment (Fig. 5M), by which time *Tbr2* was restricted to progenitors in the SVZ-RMS that give rise to Tbr1+ neuroblasts (Brill et al. 2009). Thirty days after tamoxifen induction, Tbr2+ cells were effectively eliminated from the SVZ-RMS in *Nestin*-CreER^{T2};*Tbr2*$^{Flox/Flox}$ animals (95% decrease; Control = 1860 ± 83 Tbr2+ cells; *Nestin*-CreER^{T2};*Tbr2*$^{Flox/Flox}$ = 94 ± 31 Tbr2+ cells; *t*-test, $p<0.001$) (Fig. 5N, O), suggesting efficient ablation of *Tbr2*. In contrast to embryonic and perinatal development, the total number of Tbr1+ cells in the SVZ-RMS was significantly decreased in *Nestin*-CreER^{T2};*Tbr2*$^{Flox/Flox}$ mice (Control = 1586 ± 64 Tbr1+ cells; *Nestin*-CreER^{T2};*Tbr2*$^{Flox/Flox}$ = 154 ± 31 Tbr1+ cells; *t*-test, $p<0.001$; Fig. 5T). Taken together, these results imply that *Tbr2* is important for the generation of glutamatergic neuroblasts from the adult SVZ-RMS, but is dispensable for this process during development. While we do not currently know why *Tbr2* might be differentially required during distinct periods of glutamatergic neurogenesis from the SVZ-RMS, it is possible that variances in cell intrinsic programs or extracellular signaling environments may be a factor. Evidence from other CNS regions supports this assertion. For example, ablation of *Tbr2* in the embryonic neocortex only modestly effects the production of cortical projection neurons (Arnold et al. 2008; Sessa et al. 2008), whereas knockout of *Tbr2* during hippocampal neurogenesis results in a substantial decrease in granule neuron generation (Hodge et al. 2012b, 2013).

In summary, we have described the phenotypes generated by conditional ablation of *Tbr2* in both the developing SVZ-RMS-OB and the adult SVZ-RMS. Our results show that *Tbr2* is important for the generation of mitral cells during early OB development. In the absence of *Tbr2*, this cell population is greatly decreased as evidenced by loss of the mitral cell markers Tbx21 and Reelin. Furthermore, we describe a novel SVZ-RMS defect in *Nestin*-Cre;*Tbr2*$^{Flox/Flox}$ conditional mutants that involves transient expansion of this zone accompanied by ectopic accumulation of several different kinds of cells that normally traverse this region *en route* to the OB. Lastly, we suggest that the requirement for *Tbr2*

during the generation of glutamatergic neuroblasts from the SVZ-RMS differs between embryonic/perinatal and adult neurogenesis, such that *Tbr2* is dispensable for this process in the developing SVZ-RMS but appears to be required for the generation of these cells in the adult.

Experimental Procedures

Animals

Mice were housed in an ALAAC-approved facility at Seattle Children's Research Institute (SCRI), and the Institutional Animal Care and Use Committee at SCRI approved all animal procedures. *Tbr2*^{Flox}, *Nestin*-Cre, *Nestin*-CreER^{T2}, and *Tbr2*^{LacZ} mice have been previously described (Tronche et al. 1999; Russ et al. 2000; Imayoshi et al. 2006; Intlekofer et al. 2008). All animals were maintained on a C57Bl/6 background, and both male and female animals were used for experiments. Embryonic animals were generated by timed matings, with the day of the vaginal plug considered embryonic day (E) 0.5. Embryonic brains were removed from the skull and fixed in 4% paraformaldehye for 2–4 hours, as described (Hodge et al. 2013). Postnatal and adult animals were anesthetized with Avertin (Sigma) and transcardially perfused with 4% paraformaldehyde as described (Hodge et al. 2012b). For *Nestin*-Cre, controls were *Nestin*-Cre;*Tbr2*$^{Flox/+}$ and *Tbr2* conditional knockouts were *Nestin*-Cre;*Tbr2*$^{Flox/Flox}$. For experiments using *Nestin*-CreER^{T2}, controls were *Nestin*-CreER^{T2};*Tbr2*$^{Flox/+}$, and inducible conditional *Tbr2* knockouts were *Nestin*-CreER^{T2};*Tbr2*$^{Flox/Flox}$. For experiments using the *Tbr2*^{LacZ} allele, controls were *Tbr2*$^{+/LacZ}$ and conditional *Tbr2* knockouts were Nestin-Cre;*Tbr2*$^{Flox/LacZ}$.

Tissue preparation and immunohistochemistry

After fixation, brains were cryoprotected in 30% sucrose and embedded in OCT compound (Sakura Finetek). Embryonic/early postnatal brains were sectioned at 12–16μm on a cryostat, mounted on Superfrost Plus glass slides (Fisher Scientific), and stored at −80 °C. Adult brains were fixed overnight in 4% PFA and sectioned at 40μm free floating and transferred to cryoprotectant solution, as described (Hodge et al. 2008, 2012b). Primary antibodies used in this study were: Tbr2 (rabbit, 1:1000, R. F. Hevner), Tbr1 (rabbit, 1:1500, R.F. Hevner), Tbx21 (rabbit, 1:10000, S. Stifani, McGill University), Tuj1 (mouse, 1:1000, Covance), Pax6 (mouse, 1:1000, Developmental Studies Hybridoma Bank), GFAP (rabbit, 1:1000, Dako), Doublecortin (DCX, goat, 1:400, Santa Cruz Biotechnology), Reelin (mouse, 1:1,000, Calbiochem), and activated caspase-3 (rabbit, 1:500, Cell Signaling Technologies). Sections were processed as described (Hodge et al. 2008, 2012b, 2013).

X-Gal staining

For experiments utilizing *Tbr2*^{LacZ} mice, sagittal slide mounted cryostat sections were prepared as above. Slides were then allowed to air dry, and subsequently washed three times for 5 minutes per wash in wash buffer (1X PBS; 2mM $MgCl_2$; 0.01% Deoxycholate; 0.02% NP-40). Sections were then incubated overnight at 37°C in freshly made X-Gal staining solution (wash buffer plus 5mM potassium ferrocyanide, 5mM potassium hexacyanoferrate, and 1mg/ml X-Gal; Promega). Finally, sections were washed in 1X PBS, counterstained with Nuclear Fast Red (Sigma), and coverslipped in Permount (Fisher Scientific).

Tamoxifen treatment

Tamoxifen (Sigma) was dissolved in corn oil (Fisher Scientific) at a concentration of 25 mg/ml. 8-week-old animals received tamoxifen (180mg/kg/dose, i.p.) daily for 5 consecutive days, and were then allowed to rest for 1 week. After 1 week, animals received 2 additional tamoxifen injections (180 mg/kg/day) on consecutive days, exactly as described in (Hodge et al. 2012b). Animals were collected 30 days after the last tamoxifen dose when they were 14 weeks old.

Cell counting

Images were obtained using a Zeiss LSM 710 confocal microscope (40X, 1.3 N.A. oil objective). Cell counts were conducted on N=3 animals per group. Using a modification of the optical disector principle (Gundersen et al. 1988), counts of Tbr2+ and Tbr1+ cells were conducted on every 6^{th} 40 μm sagittal section through the entire rostrocaudal extent of the SVZ-RMS from the entry of the RMS into the core of the OB to the caudal tip of the lateral ventricle (Bregma +3.5mm to −3mm). Cells intersecting the top-plane of focus were excluded from counts.

Statistical analyses

Statistical analyses were conducted using a two-sample t-test with SPSS statistical software (IBM). Differences were considered statistically significant at $p<0.05$.

Acknowledgments

Thomas Walsh, Ray Daza, Diane Pham, and Kristin Mussar provided technical assistance. We thank Dr. Branden Nelson for helpful discussions and advice on experimental design. Dr. Steven Reiner (Columbia University) generated the *Tbr2* conditional allele, and we thank him for generously sharing this resource. Dr. Ryoichiro Kageyama (Kyoto University) kindly provided the *Nestin*-CreER^{T2} mice. This work was supported by Grant NIH 1R01MH080766 to Dr. Robert F. Hevner. Dr. Robert J. Kahoud was a NICHD fellow of the Pediatric Scientist Development Program (NIH K12 HD000850).

References

Allen ZJ, Waclaw RR, Colbert MC, Campbell K. Molecular identity of olfactory bulb interneurons: transcriptional codes of periglomerular neuron subtypes. J Mol Hist. 2007; 38:517–525.

Arnold SJ, Huang G-J, Cheung AF, Era T, Nishikawa S-I, Bikoff EK, Molnar Z, Robertson EJ, Groszer M. The T-box transcription factor Eomes/Tbr2 regulates neurogenesis in the cortical subventricular zone. Genes Dev. 2008; 22:2479–2484. [PubMed: 18794345]

Batista-Brito R, Close J, Machold R, Fishell G. The distinct temporal origins of olfactory bulb interneuron subtypes. J Neurosci. 2008; 28:3966–3975. [PubMed: 18400896]

Blanchart A, De Carlos JA, López-Mascaraque L. Time frame of mitral cell development in the mice olfactory bulb. J Comp Neurol. 2006; 496:529–543. [PubMed: 16572431]

Brill MS, Ninkovic J, Winpenny E, Hodge RD, Ozen I, Yang R, Lepier A, Gascón S, Erdelyi F, Szabo G, Parras C, Guillemot F, Frotscher M, Berninger B, Hevner RF, Raineteau O, Götz M. Adult generation of glutamatergic olfactory bulb interneurons. Nat Neurosci. 2009; 12:1524–1533. [PubMed: 19881504]

Bulfone A, Martinez S, Marigo V, Campanella M, Basile A, Quaderi N, Gattuso C, Rubenstein JL, Ballabio A. Expression pattern of the *Tbr2* (*Eomesodermin*) gene during mouse and chick brain development. Mech Dev. 1999; 84:133–138. [PubMed: 10473127]

Couillard-Despres S, Winner B, Schaubeck S, Aigner R, Vroemen M, Weidner N, Bogdahn U, Winkler J, Kuhn H-G, Aigner L. Doublecortin expression levels in adult brain reflect neurogenesis. Eur J Neurosci. 2005; 21:1–14. [PubMed: 15654838]

De Marchis S, Bovetti S, Carletti B, Hsieh Y-C, Garzotto D, Peretto P, Fasolo A, Puche AC, Rossi F. Generation of Distinct Types of Periglomerular Olfactory Bulb Interneurons during Development and in Adult Mice: Implication for Intrinsic Properties of the Subventricular Zone Progenitor Population. J Neurosci. 2007; 27:657–664. [PubMed: 17234597]

Elsen GE, Hodge RD, Bedogni F, Daza RAM, Nelson BR, Shiba N, Reiner SL, Hevner RF. The protomap is propagated to cortical plate neurons through an Eomes-dependent intermediate map. Proc Natl Acad Sci USA. 2013; 110:4081–4086. [PubMed: 23431145]

Englund C, Fink A, Lau C, Pham D, Daza RAM, Bulfone A, Kowalczyk T, Hevner RF. Pax6, Tbr2, and Tbr1 are expressed sequentially by radial glia, intermediate progenitor cells, and postmitotic neurons in developing neocortex. J Neurosci. 2005; 25:247–251. [PubMed: 15634788]

Faedo A, Ficara F, Ghiani M, Aiuti A, Rubenstein JLR, Bulfone A. Developmental expression of the T-box transcription factor T-bet/Tbx21 during mouse embryogenesis. Mech Dev. 2002; 116:157–160. [PubMed: 12128215]

Gong Q, Shipley MT. Evidence that pioneer olfactory axons regulate telencephalon cell cycle kinetics to induce the formation of the olfactory bulb. Neuron. 1995; 14:91–101. [PubMed: 7826645]

Gundersen HJ, Bagger P, Bendtsen TF, Evans SM, Korbo L. The new stereological tools - disector, fractionator, nucleator and point sampled intercepts and their use in pathological research and diagnosis. APMIS. 1988; 96:857–881. [PubMed: 3056461]

Hack I, Bancila M, Loulier K, Carroll P, Cremer H. Reelin is a detachment signal in tangential chain-migration during postnatal neurogenesis. Nat Neurosci. 2002; 5:939–945. [PubMed: 12244323]

Hellwig S, Hack I, Zucker B, Brunne B, Junghans D. Reelin together with ApoER2 regulates interneuron migration in the olfactory bulb. PLoS ONE. 2012; 7:e50646. [PubMed: 23209795]

Hodge RD, Kowalczyk TD, Wolf S, Encinas J, Rippey C, Enikolopov G, Kempermann G, Hevner RF. Intermediate progenitors in adult hippocampal neurogenesis: Tbr2 expression and coordinate regulation of neuronal output. J Neurosci. 2008; 28:3707–3717. [PubMed: 18385329]

Hodge RD, Hevner RF. Expression and actions of transcription factors in adult hippocampal neurogenesis. Dev Neurobiol. 2011; 71:680–689. [PubMed: 21412988]

Hodge RD, Garcia AJ, Elsen GE, Nelson BR, Mussar KE, Reiner SL, Ramirez J-M, Hevner RF. Tbr2 expression in Cajal-Retzius cells and intermediate neuronal progenitors is required for morphogenesis of the Dentate Gyrus. J Neurosci. 2013; 33:4165–4180. [PubMed: 23447624]

Hodge RD, Kahoud RJ, Hevner RF. Transcriptional control of glutamatergic differentiation during adult neurogenesis. Cell Mol Life Sci. 2012a; 69:2125–2134. [PubMed: 22249196]

Hodge RD, Nelson BR, Kahoud RJ, Yang R, Mussar KE, Reiner SL, Hevner RF. Tbr2 Is essential for hippocampal lineage progression from neural stem cells to intermediate progenitors and neurons. J Neurosci. 2012b; 32:6275–6287. [PubMed: 22553033]

Hsieh J. Orchestrating transcriptional control of adult neurogenesis. Genes Dev. 2012; 26:1010–1021. [PubMed: 22588716]

Imamura F, Ayoub AE, Rakic P, Greer CA. Timing of neurogenesis is a determinant of olfactory circuitry. Nat Neurosci. 2011; 14:331–337. [PubMed: 21297629]

Imayoshi I, Ohtsuka T, Metzger D, Chambon P, Kageyama R. Temporal regulation of Cre recombinase activity in neural stem cells. Genesis. 2006; 44:233–238. [PubMed: 16652364]

Intlekofer AM, Banerjee A, Takemoto N, Gordon SM, DeJong CS, Shin H, Hunter CA, Wherry EJ, Lindsten T, Reiner SL. Anomalous type 17 response to viral infection by CD8+ T Cells lacking T-bet and Eomesodermin. Science. 2008; 321:408–411. [PubMed: 18635804]

Kohwi M, Petryniak MA, Long JE, Ekker M, Obata K, Yanagawa Y, Rubenstein JLR, Alvarez-Buylla A. A subpopulation of olfactory bulb GABAergic interneurons is derived from Emx1- and Dlx5/6-expressing progenitors. J Neurosci. 2007; 27:6878–6891. [PubMed: 17596436]

Lledo P, Merkle F, Alvarezbuylla A. Origin and function of olfactory bulb interneuron diversity. Trends Neurosci. 2008; 31:392–400. [PubMed: 18603310]

Lledo P-M, Saghatelyan A. Integrating new neurons into the adult olfactory bulb: joining the network, life-death decisions, and the effects of sensory experience. Trends Neurosci. 2005; 28:248–254. [PubMed: 15866199]

Merkle FT, Mirzadeh Z, Alvarez-Buylla A. Mosaic organization of neural stem cells in the adult brain. Science. 2007; 317:381–384. [PubMed: 17615304]

Mizuguchi R, Naritsuka H, Mori K, Yoshihara Y. Tbr2 deficiency in mitral and tufted cells disrupts excitatory-inhibitory balance of neural circuitry in the mouse olfactory bulb. J Neurosci. 2012; 32:8831–8844. [PubMed: 22745484]

Pencea V, Luskin MB. Prenatal development of the rodent rostral migratory stream. J Comp Neurol. 2003; 463:402–418. [PubMed: 12836176]

Peretto P, Giachino C, Aimar P, Fasolo A, Bonfanti L. Chain formation and glial tube assembly in the shift from neonatal to adult subventricular zone of the rodent forebrain. J Comp Neurol. 2005; 487:407–427. [PubMed: 15906315]

Roybon L, Deierborg T, Brundin P, Li J-Y. Involvement of Ngn2, Tbr and NeuroD proteins during postnatal olfactory bulb neurogenesis. Eur J Neurosci. 2009; 29:232–243. [PubMed: 19200230]

Russ AP, Wattler S, Colledge WH, Aparicio SA, Carlton MB, Pearce JJ, Barton SC, Surani MA, Ryan K, Nehls MC, Wilson V, Evans MJ. Eomesodermin is required for mouse trophoblast development and mesoderm formation. Nature. 2000; 404:95–99. [PubMed: 10716450]

Seri B, García-Verdugo JM, Collado-Morente L, McEwen BS, Alvarez-Buylla A. Cell types, lineage, and architecture of the germinal zone in the adult dentate gyrus. J Comp Neurol. 2004; 478:359–378. [PubMed: 15384070]

Sessa A, Mao C, Hadjantonakis A, Klein W, Broccoli V. *Tbr2* directs conversion of radial glia into basal precursors and guides neuronal amplification by indirect neurogenesis in the developing neocortex. Neuron. 2008; 60:56–69. [PubMed: 18940588]

Sessa A, Mao C-A, Colasante G, Nini A, Klein WH, Broccoli V. Tbr2-positive intermediate (basal) neuronal progenitors safeguard cerebral cortex expansion by controlling amplification of pallial glutamatergic neurons and attraction of subpallial GABAergic interneurons. Genes Dev. 2010; 24:1816–1826. [PubMed: 20713522]

Shaker T, Dennis D, Kurrasch DM, Schuurmans C. Neurog1 and Neurog2 coordinately regulate development of the olfactory system. Neural Dev. 2012; 7:28. [PubMed: 22906231]

Takashima Y, Era T, Nakao K, Kondo S, Kasuga M, Smith AG, Nishikawa S-I. Neuroepithelial cells supply an initial transient wave of MSC differentiation. Cell. 2007; 129:1377–1388. [PubMed: 17604725]

Tronche F, Kellendonk C, Kretz O, Gass P, Anlag K, Orban PC, Bock R, Klein R, Schütz G. Disruption of the glucocorticoid receptor gene in the nervous system results in reduced anxiety. Nat Genet. 1999; 23:99–103. [PubMed: 10471508]

Walker TL, Yasuda T, Adams DJ, Bartlett PF. The doublecortin-expressing population in the developing and adult brain contains multipotential precursors in addition to neuronal-lineage cells. J Neurosci. 2007; 27:3734–3742. [PubMed: 17409237]

Whitman MC, Greer CA. Adult neurogenesis and the olfactory system. Prog Neurobiol. 2009; 2:162–175. [PubMed: 19615423]

Winpenny E, Lebel-Potter M, Fernandez ME, Brill MS, Gotz M, Guillemot F, Raineteau O. Sequential generation of olfactory bulb Glutamatergic neurons by Neurog2-expressing precursor cells. Neural Dev. 2011; 6:12. [PubMed: 21466690]

Key Findings

- Conditional deletion of *Tbr2* results in hypoplasia of the olfactory bulb and defects in the generation of olfactory bulb projection neurons (mitral cells).
- Development of the subventricular zone and rostral migratory stream is disrupted by *Tbr2* ablation.
- Adult glutamatergic neurogenesis from the SVZ is impaired following specific ablation of *Tbr2* in the adult brain.

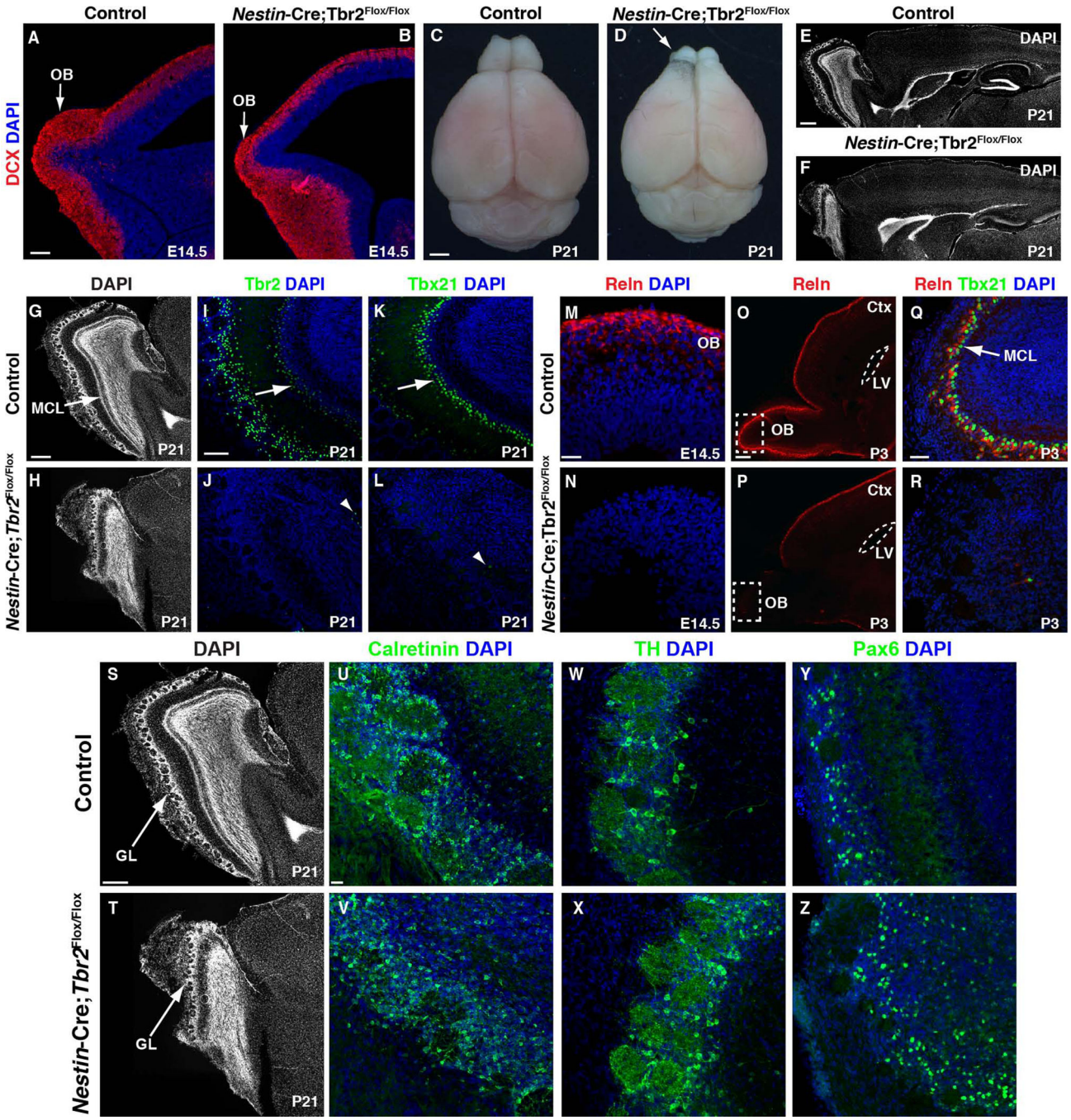

Figure 1. Conditional ablation of *Tbr2* results in OB hypoplasia and loss of mitral cells

(A) At E14.5, OB neurogenesis is well underway in control mice, as evidenced by robust expression of DCX (red, arrow). (B) In *Nestin*-Cre;*Tbr2*$^{Flox/Flox}$ animals, the OB is visibly smaller than controls by E14.5 (arrow), and there is an apparent reduction in DCX staining (red). (C–D) Gross photos of control and *Nestin*-Cre;*Tbr2*$^{Flox/Flox}$ brains at P21. (E–F) Sagittal DAPI stained sections from P21 control and *Nestin*-Cre;*Tbr2*$^{Flox/Flox}$ mice illustrate hypoplasia of the OB in mutant animals. (G–L) Mitral cells are nearly absent in *Nestin*-Cre;*Tbr2*$^{Flox/Flox}$ mice by P21. (G–H) DAPI staining illustrates gross loss of the mitral cell layer (MCL; G, arrow, compare to H) in *Tbr2* mutant mice. (I–J) Tbr2+ cells (green) are essentially absent from the MCL except for a few scattered cells (J, arrowhead) in *Nestin*-Cre;*Tbr2*$^{Flox/Flox}$ mice at P21. (K–L) Tbx21+ cells (green) are similarly

reduced in the OB of *Tbr2* mutant mice (L, arrowhead). (M–N) Consistent with decreased mitral cells, Reelin (Reln, red) staining is reduced in the OB of *Nestin*-Cre;*Tbr2*$^{Flox/Flox}$ mice as early as E14.5. (O-R) Decreased Reln expression persists through postnatal development in *Tbr2* conditional mutant mice. (P) At P3, loss of Reln is seen only in the OB of *Nestin*-Cre;*Tbr2*$^{Flox/Flox}$ mice (dashed white box), whereas Reln expression in the rest of the brain appears unaffected. (Q–R) Reln is nearly absent from mitral cells in the mutant OB at P3. Regions illustrated by dashed white boxes in O, P are shown at higher magnification in Q, R, respectively. (S–Z) Other types of OB neurons (calretinin+, tyrosine hydroxylase [TH]+, and Pax6+) appear to be relatively unaffected in number and density by loss of *Tbr2* expression in mutant mice, although general disorganization of cells within the mutant OB is apparent. (S–T) Note that the glomerular layer appears to be at least somewhat preserved in *Nestin*-Cre;*Tbr2*$^{Flox/Flox}$ mice. GL – glomerular layer, LV – lateral ventricle. Scale bars: A = 150 μm, C = 1 cm, E = 100 μm, G = 500 μm, I = 100 μm, M = 25 μm, O = 200 μm, Q = 50 μm, S = 200 μm, U = 25 μm.

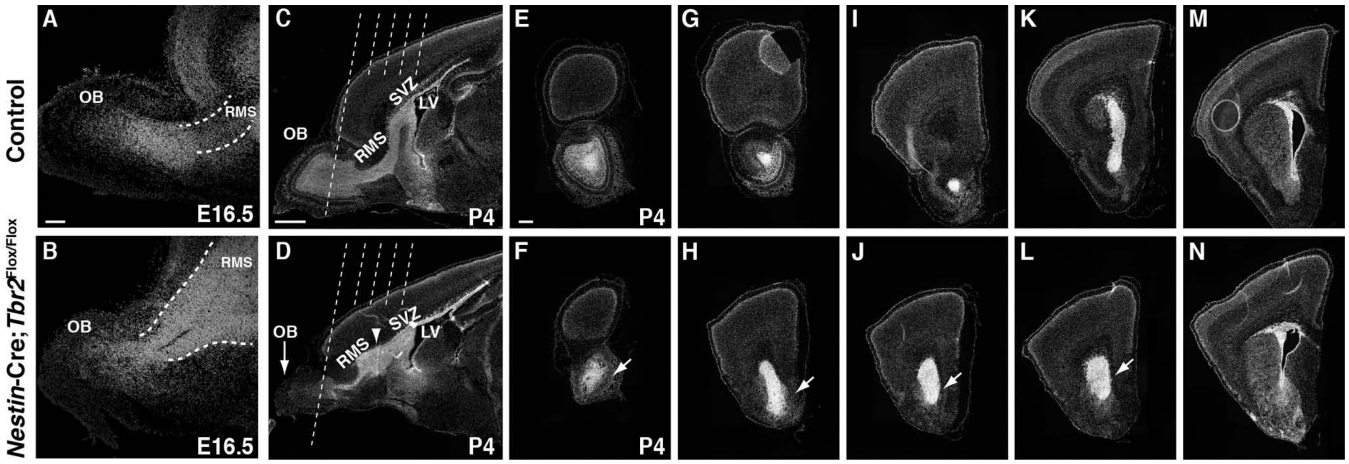

Figure 2. The SVZ-RMS is expanded in embryonic and perinatal *Nestin*-Cre;*Tbr2*$^{Flox/Flox}$ mice

(A–B) Expansion of the SVZ-RMS is apparent in *Nestin*-Cre;*Tbr2*$^{Flox/Flox}$ as early as E16.5. (B) Increased cellular density is apparent within the mutant RMS. (C–D) Low magnification images of representative sagittal sections through the SVZ-RMS in control (C) and *Nestin*-Cre;*Tbr2*$^{Flox/Flox}$ (D) mice at P4 show expansion of the SVZ-RMS in *Tbr2* mutant mice. Dashed lines in C and D correspond to the levels of coronal sections shown in adjacent panels. (E–N) Coronal sections from mid OB to anterior SVZ further illustrate gross expansion of the SVZ-RMS in P4 *Nestin*-Cre;*Tbr2*$^{Flox/Flox}$ mice. LV – lateral ventricle. Scale bars: A = 100 μm, C = 500 μm, E = 500 μm.

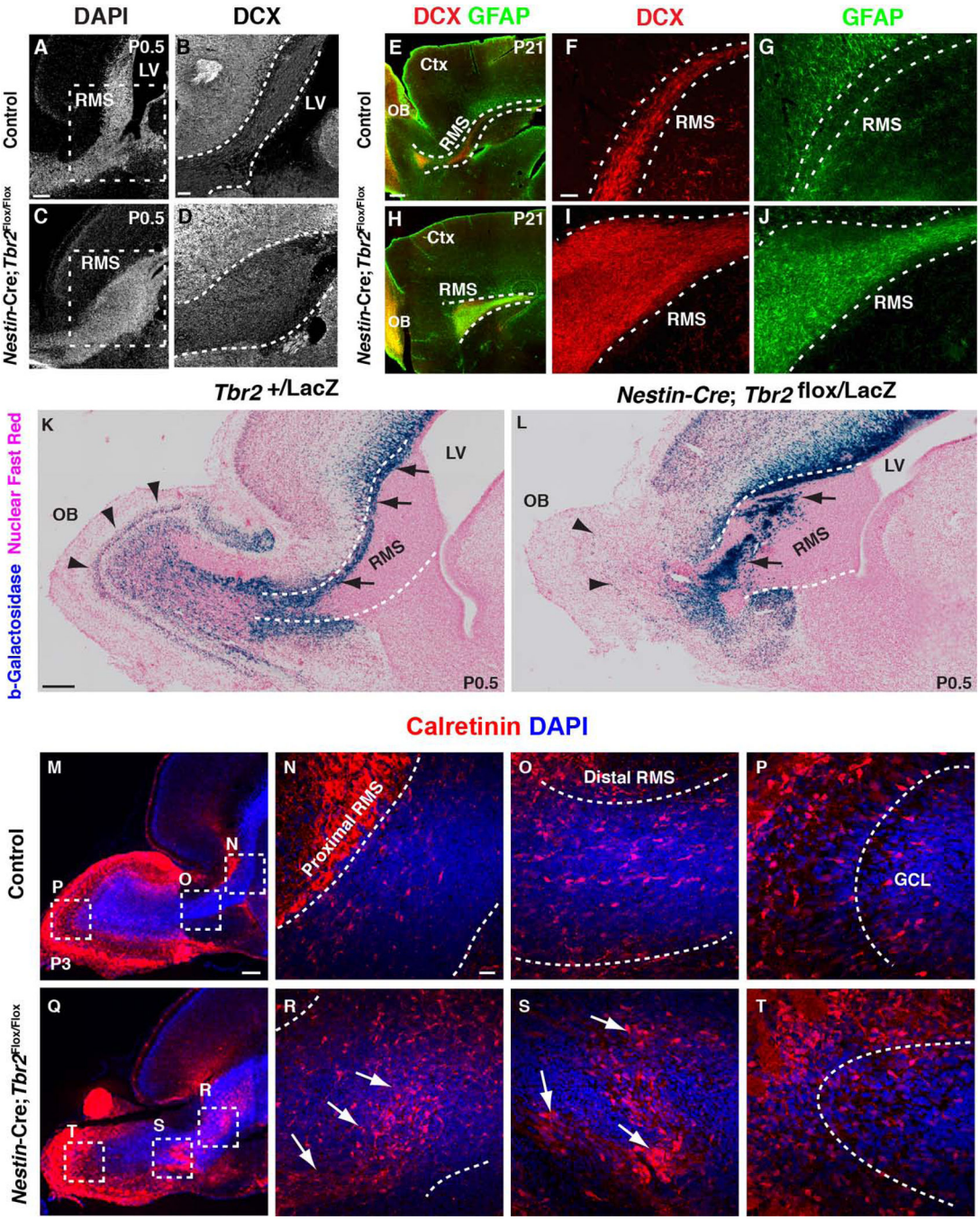

Figure 3. Ectopic accumulation of different types of cells within the expanded SVZ-RMS of *Nestin*-Cre;*Tbr2*$^{Flox/Flox}$ mice

(A, C) DAPI staining illustrates expansion of the SVZ-RMS in Tbr2 mutant mice at P0.5. (B, D) Ectopic accumulation of neuroblasts (DCX+) is apparent within the SVZ-RMS of *Nestin*-Cre;*Tbr2*$^{Flox/Flox}$ mice on P0.5. Regions illustrated by dashed boxes in A, C are shown in higher magnification in B, D, respectively. (E–J) The expanded *Tbr2* mutant RMS contains both neuroblasts (DCX+, red) and glial cells (GFAP+, green), as illustrated on P21. (E, H) Lower magnification images of sagittal sections illustrate the expanded RMS in *Nestin*-Cre;*Tbr2*$^{Flox/Flox}$ mice at P21 (compare white dashed lines in E and H). (K–L) In *Nestin*-Cre;Tbr2$^{Flox/LacZ}$ mice, abnormal enlargement of the proximal RMS is apparent by P0.5 as is ectopic accumulation of β-galactosidase+ cells within the RMS (L, arrows). Few β-galactosidase+ cells are apparent in the mutant OB (L, arrowheads). (K)

Comparatively, in controls most β-galactosidase+ cells are located in the either the core of the OB or in the MCL (black arrowheads), although some are still present within the RMS (black arrows). (M–T) Calretinin+ (red) neuroblasts are also present within the expanded SVZ-RMS of *Nestin*-Cre;*Tbr2*$^{Flox/Flox}$ mice, as illustrated at P3. Regions in dashed boxes in M and Q are shown at higher magnification in the adjacent marked panels. Note that ectopic accumulation of calretinin+ cells is apparent in both the proximal (compare N and R) and distal (compare O and S) branches of the mutant RMS. (P, T) Calretinin+ cells also appear disorganized in the OB of *Nestin*-Cre;*Tbr2*$^{Flox/Flox}$ mice. Scale bars: A = 200 μm, B = 50 μm, E = 500 μm, F = 100 μm, K = 500 μm, M = 100 μm, N = 50 μm.

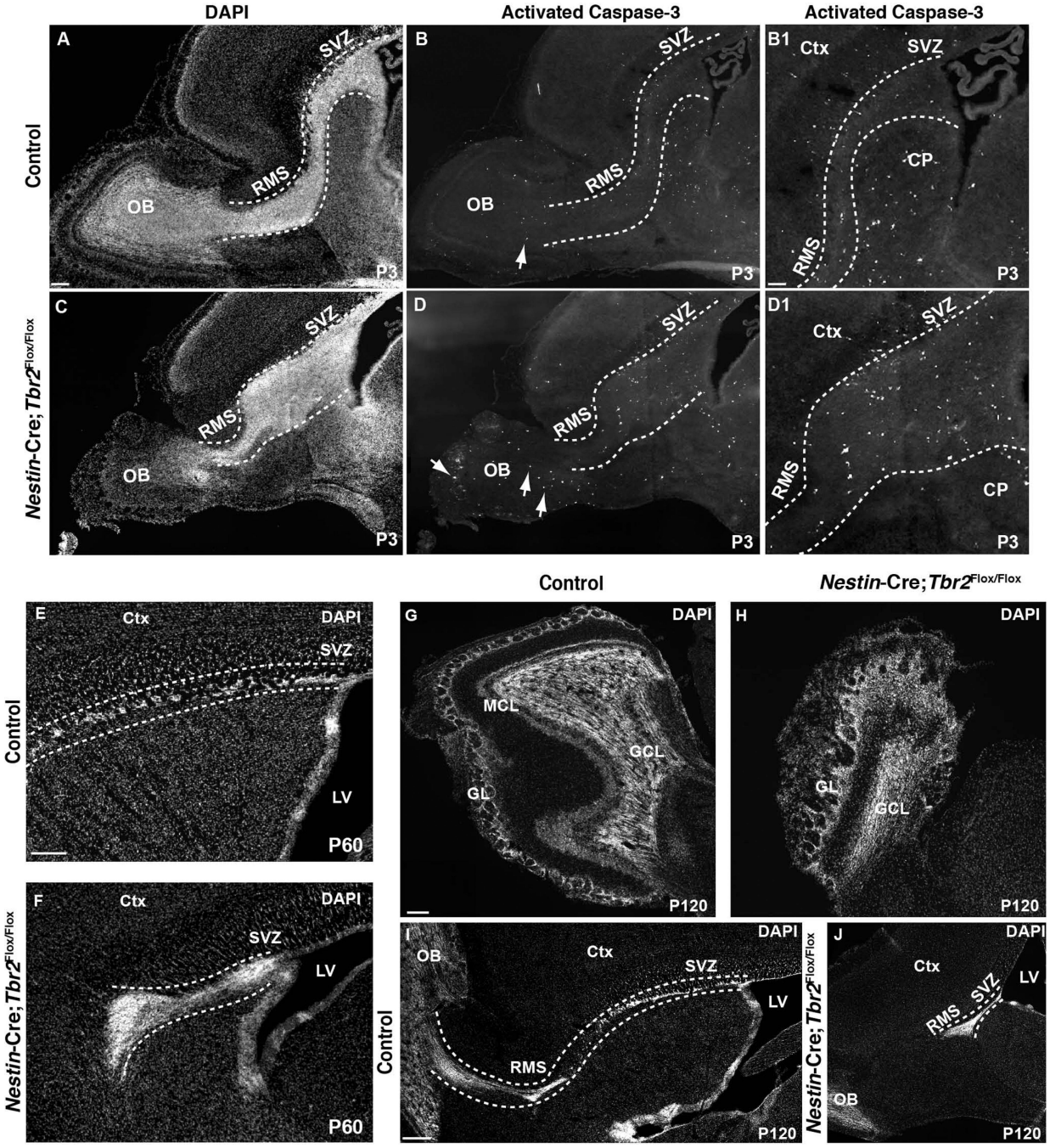

Figure 4. Cell death is increased in the SVZ-RMS-OB of *Nestin*-Cre;*Tbr2*$^{Flox/Flox}$ mice, and by adulthood, expansion of the SVZ-RMS is less apparent in mutant mice

(A–D) Activated caspase-3 immunostaining reveals an apparent increase in cell death in the SVZ-RMS-OB of *Nestin*-Cre;*Tbr2*$^{Flox/Flox}$ mice during early postnatal development (P3; arrows; compare B1 and D1). DAPI staining is shown in A, C to provide context for the images of activated caspase-3 immunostaining in B–B1, D–D1. Images shown in B1 and D1 are higher magnification views of B and D, respectively. (E–F) By P60, expansion of the SVZ-RMS is somewhat reduced compared to earlier stages in *Tbr2* mutant mice, although the RMS is still abnormal as it does not appear to properly connect to the OB in mutants (dashed white lines in F). (G–H) In adult (P120) *Nestin*-Cre;*Tbr2*$^{Flox/Flox}$ mice, hypoplasia of the OB continues to be

apparent. Similar to younger animals, loss of the MCL is notable in mutant mice, as is disorganization of the OB in general (H). (I–J) In adult controls, the SVZ-RMS is easily identifiable and can be seen entering the OB (I, dashed white lines). Conversely in adult *Nestin*-Cre;*Tbr2*$^{Flox/Flox}$ mice, the SVZ-RMS is slightly wider and the RMS is truncated and does not appear to enter the OB (J, white dashed lines). GCL – granule cell layer, GL – glomerular layer, Ctx – cerebral cortex, CP – caudate putamen, LV – lateral ventricle. Scale bars: A = 100 μm, B1 = 50 μm, E = 150 μm, G = 100 μm, I = 200 μm.

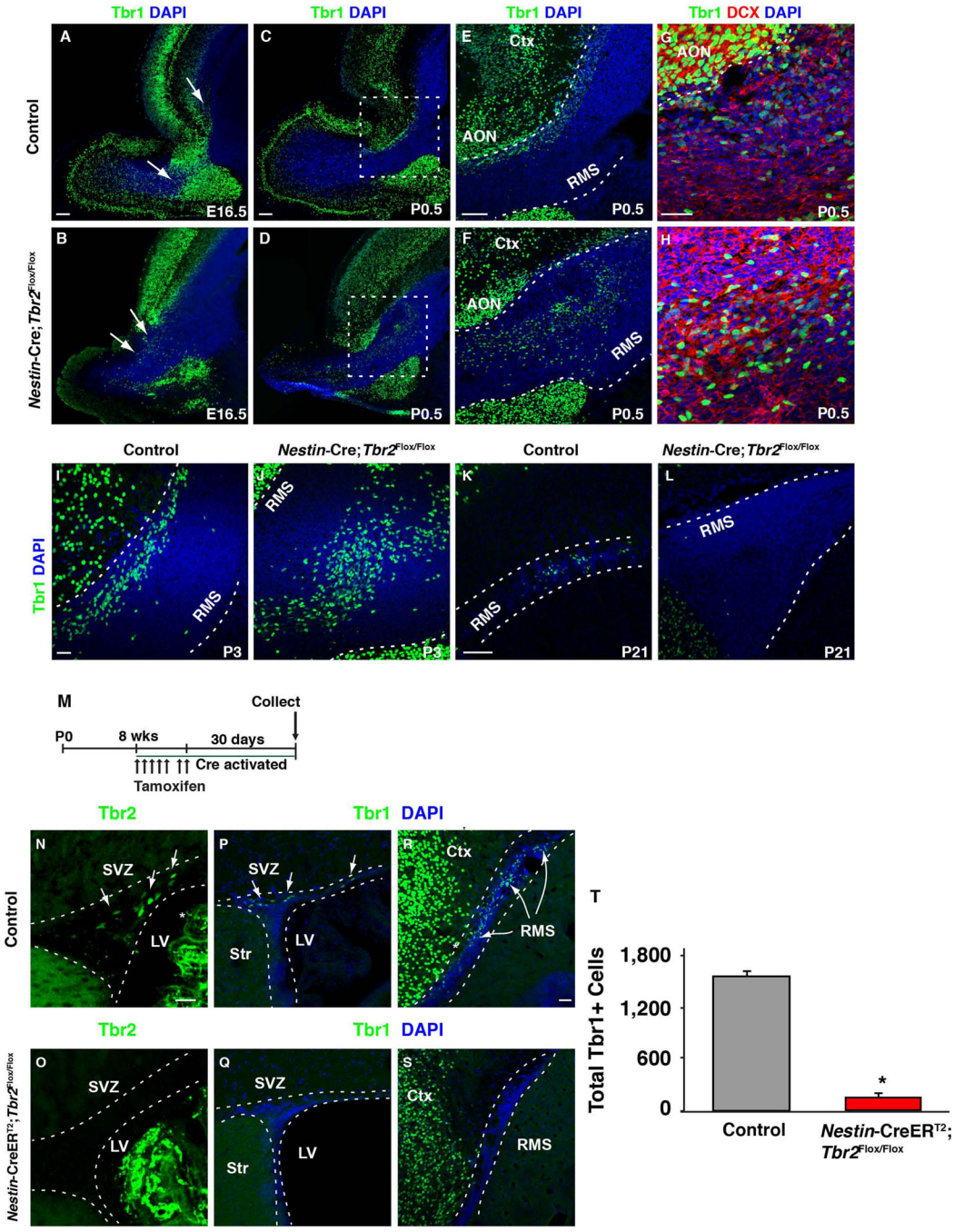

Figure 5. Differential effects of conditional ablation of *Tbr2* on glutamatergic neurogenesis during embryonic/perinatal development and adult neurogenesis

(A–L) Tbr1 identifies different migratory glutamatergic neuroblast populations generated from progenitors in the SVZ throughout development. (A, C, E, G, I, K) Tbr1 is expressed in the RMS of controls from E16.5 through to P21. Coexpression of DCX (red) is apparent in many Tbr1+ cells at P0.5, suggesting that most of these cells are migrating neuroblasts (G) in control mice. (B) In E16.5 *Nestin*-Cre;*Tbr2*$^{flox/flox}$ mice, Tbr1+ cells are present but they are ectopically located in the RMS (arrows). (C–H) At P0.5, ectopic Tbr1+ cells are still apparent in the mutant RMS, suggesting that loss of *Tbr2* does not impact the generation of these cells. (H) Many of the Tbr1+ cells that accumulate in the RMS of *Tbr2* mutant mice coexpress DCX

(red), suggesting that they are migratory neuroblasts. Accumulation of Tbr1+ cells persists in the RMS of *Nestin*-Cre;*Tbr2*$^{flox/flox}$ mice through the first postnatal week (compare I and J). However, by P21, Tbr1+ cells are essentially absent from the RMS in *Nestin*-Cre;*Tbr2*$^{flox/flox}$ mice (L). Comparatively, Tbr1+ cells are present in the P21 control RMS (K). Note that Tbr1 is expressed by mature neurons in the anterior olfactory nucleus (AON) as well as the cortex throughout development (see E, F, G). (M) Schematic diagram illustrating tamoxifen dosing schedule for conditional ablation of *Tbr2* in *Nestin*-CreER^{T2};*Tbr2*$^{flox/flox}$ mice during adult glutamatergic neurogenesis. (N–O) Tbr2 protein (green) is effectively ablated from the SVZ of adult *Nestin*-CreER^{T2};*Tbr2*$^{flox/flox}$ mice 30 days after the end of tamoxifen dosing. Note that there is non-specific staining of the choroid plexus in both controls and mutants (white asterisk, N). In controls (P, R), Tbr1+ glutamatergic neuroblasts are present in both the SVZ (R) and RMS (R), whereas in *Nestin*-CreER^{T2};*Tbr2*$^{flox/flox}$ mice, Tbr1+ cells are essentially absent from both of these regions (Q, S). (T) Quantification of the decrease in Tbr1+ cells in *Nestin*-CreER^{T2};*Tbr2*$^{flox/flox}$ mice during adult neurogenesis (*p<0.001, *t*-test). Graph illustrates the mean ± SEM for each group. LV – lateral ventricle, Str – striatum, Ctx – cerebral cortex. Scale bars: A, C, E = 100 μm, G, I = 50 μm, K = 100 μm, N, R = 25 μm.